

Unified Analysis of Spin Isospin Responses of Nuclei

T. Wakasa,¹ M. Ichimura,² and H. Sakai³

¹*Department of Physics, Kyushu University, Higashi, Fukuoka 812-8581, Japan*

²*Faculty of Computer and Information Sciences,
Hosei University, Koganei, Tokyo 184-8584, Japan*

³*Department of Physics, The University of Tokyo, Bunkyo, Tokyo 113-0033, Japan*

(Dated: November 20, 2018)

Abstract

We investigated the Gamow-Teller (GT) strength distribution, especially the quenching with respect to the GT sum rule, and the enhancement of the pionic responses in the quasielastic scattering region, in the same theoretical framework. That is the continuum random phase approximation with the $\pi + \rho + g'$ model interaction, incorporated with distorted wave impulse approximation and two-step calculations. From this analysis we searched the Landau-Migdal parameters, g'_{NN} and $g'_{N\Delta}$, through the comparison with the experimental data of the GT strength distribution obtained at 300 MeV and the spin-longitudinal (pionic) cross sections ID_q of (\vec{p}, \vec{n}) at 350 and 500 MeV. This comprehensive and sophisticated study gave a common set of $g'_{NN}=0.6-0.7$ and $g'_{N\Delta}=0.2-0.4$, for both low and high momentum transfers.

PACS numbers: 21.30.Fe, 21.60.Jz, 25.40.Kv, 24.30.Cz

Recent (p, n) and (n, p) experiments at intermediate energies have presented reliable information on nuclear spin isospin responses [1]. Following two contrastive subjects are especially interesting. One is quenching of the total strength of the Gamow-Teller (GT) transitions [2] from its sum rule value $3(N-Z)$ [3], and the other is enhancement of the pionic (isovector spin-longitudinal) response functions in the quasielastic scattering (QES) region [4, 5, 6] as a precursor of the pion condensation [7]. A common key concept to understand these contrastive phenomena simultaneously is the Landau-Migdal (LM) parameters, g'_{NN} , $g'_{N\Delta}$, and $g'_{\Delta\Delta}$, which specify the LM interactions V_{LM} , namely the zero range particle-hole (ph) and Delta-hole (Δh) interactions.

In this paper we study the GT strength distributions and the quenching factor observed at 295 MeV at RCNP, and the spin-longitudinal cross sections ID_q of (\vec{p}, \vec{n}) at 346 MeV at RCNP and at 494 MeV at LAMPF, which well represent the pionic response function R_L . To all these observables, we apply the same theoretical framework, namely the continuum random phase approximation (RPA) with the $\pi + \rho + g'$ model interaction, which properly treats the finite geometry. Then we look for the LM parameters, which reproduce the data as well as possible.

Estimations of g'_{NN} from the GT giant resonances (GTGR) have been carried out by several authors [8]. For instance, Suzuki [9] used energy weighted sum technique and Bertsch, Cha, and Toki [10] used the continuum RPA. Fitting the peak position of GTGR, they obtained similar values of $g'_{NN} \approx 0.6$ for ^{90}Zr . Their analyses used only the LM interaction for the nucleons. Most of later works with Δ [11, 12] used the universality ansatz, $g'_{NN} = g'_{N\Delta} = g'_{\Delta\Delta}$. Further the experimental spectra are of the cross sections of (p, n) , but not of the genuine GT strength. We re-investigate the GTGR spectrum by use of $\pi + \rho + g'$ model interaction without the universality ansatz.

From the GT quenching factor, Suzuki and Sakai [13] estimated $g'_{N\Delta}$ by the Fermi gas model only with V_{LM} , treating the finite size effect crudely. They obtained $g'_{N\Delta} \approx 0.2$ for ^{90}Zr . Using the first order perturbation on the $N\Delta$ transition part of the $\pi + \rho + g'$ model interaction, Arima *et al.* [14] obtained $g'_{N\Delta} \approx 0.3$. This increase of 0.1 from the Suzuki-Sakai's result comes from the π and ρ exchange interaction due to the nuclear finite size. The present RPA calculation presents more integrated analysis.

As to the pionic responses in the QES region, it has been shown [15] that a conventionally used eikonal approximation is not quantitatively reliable to extract the pionic response

function R_L from ID_q due to the nuclear distortion. Thus we have to calculate ID_q by the distorted wave impulse approximation (DWIA) incorporated with the continuum RPA response functions, and to compare the theoretical and experimental results directly. Further it has also been shown [6] that two-step processes contribute as an appreciable background for the RCNP data. Therefore we extend the DWIA + two-step analysis to the LAMPF data and search the suitable g' 's in an overall point of view.

We write the $\beta^\pm(\text{GT}^\pm)$ transition operators with N and Δ in the unit of g_A as

$$O_{\text{GT}}^\pm = \mp \frac{1}{\sqrt{2}} \sum_{k=1}^A \left\{ \tau_{k,\pm 1} \boldsymbol{\sigma}_k + \frac{g_A^{N\Delta}}{g_A} \left(T_{k,\pm 1} \mathbf{S}_k - T_{k,\mp 1}^\dagger \mathbf{S}_k^\dagger \right) \right\}, \quad (1)$$

with $\tau_{\pm 1} = \mp \frac{1}{\sqrt{2}}(\tau_x \pm i\tau_y)$ and $T_{\pm 1} = \mp \frac{1}{\sqrt{2}}(T_x \pm iT_y)$, where $g_A(g_A^{N\Delta})$ is the weak coupling constant for NN ($N\Delta$) transition, and $\boldsymbol{\sigma}(\boldsymbol{\tau})$ is the nucleon Pauli spin (isospin) matrix, and $\mathbf{S}(\mathbf{T})$ is the spin (isospin) transition operator from N to Δ . Similarly we write the isovector spin-longitudinal transition operators with momentum transfer \mathbf{q} as

$$O_L^\lambda(\mathbf{q}) = \sum_{k=1}^A \left\{ \tau_{k,\lambda} \boldsymbol{\sigma}_k \cdot \hat{\mathbf{q}} + \frac{f_{\pi N\Delta}}{f_{\pi NN}} \left(T_{k,\lambda} \mathbf{S}_k \cdot \hat{\mathbf{q}} + (-1)^\lambda T_{k,-\lambda}^\dagger \mathbf{S}_k^\dagger \cdot \hat{\mathbf{q}} \right) \right\} e^{i\mathbf{q} \cdot \mathbf{r}_k}, \quad (2)$$

where $\lambda = 0, \pm 1$, and $f_{\pi NN}(f_{\pi N\Delta})$ is the $\pi NN(\pi N\Delta)$ coupling constant. Here we neglect the transitions from Δ to Δ in both O_{GT}^\pm and $O_L^\lambda(\mathbf{q})$. We take the quark model relation $f_{\pi N\Delta}/f_{\pi NN} = g_A^{N\Delta}/g_A = \sqrt{72/25} \simeq 1.70$ in this paper. What we are interested in are how the nuclei respond to these operators.

Since neither the momentum \mathbf{q} nor the spin directions are conserved in finite nuclei, we introduce the spin-isospin transition densities

$$O_{\lambda,a}^N(\mathbf{r}) = \sum_{k=1}^A \tau_{k,\lambda} \sigma_{k,a} \delta(\mathbf{r} - \mathbf{r}_k), \quad O_{\lambda,a}^\Delta(\mathbf{r}) = \sum_{k=1}^A T_{k,\lambda} S_{k,a} \delta(\mathbf{r} - \mathbf{r}_k), \quad (3)$$

with $a = x, y, z$, and calculate the spin-isospin response functions

$$R_{\lambda,ba}^{\alpha\beta}(\mathbf{r}', \mathbf{r}, \omega) = \sum_n \langle \Psi_0 | O_{\lambda,b}^{\alpha\dagger}(\mathbf{r}') | \Psi_n \rangle \langle \Psi_n | O_{\lambda,a}^\beta(\mathbf{r}) | \Psi_0 \rangle \delta(\omega - (\mathcal{E}_n - \mathcal{E}_0)), \quad (4)$$

by the continuum RPA with the orthogonality condition in the coordinate representation [16].

The $\pi + \rho + g'$ model interaction is written as

$$V^{\text{eff}}(\mathbf{q}, \omega) = V_{\text{LM}} + V_\pi(\mathbf{q}, \omega) + V_\rho(\mathbf{q}, \omega), \quad (5)$$

where V_π and V_ρ are the one-pion and the one-rho-meson exchange interactions, respectively. The LM interaction V_{LM} is written by the LM parameters g'_{NN} , $g'_{N\Delta}$, $g'_{\Delta\Delta}$ as

$$\begin{aligned} V_{\text{LM}} = & \frac{f_{\pi NN}^2}{m_\pi^2} g'_{NN} (\boldsymbol{\tau}_1 \cdot \boldsymbol{\tau}_2) (\boldsymbol{\sigma}_1 \cdot \boldsymbol{\sigma}_2) \\ & + \frac{f_{\pi NN} f_{\pi N\Delta}}{m_\pi^2} g'_{N\Delta} \left\{ (\boldsymbol{\tau}_1 \cdot \mathbf{T}_2) (\boldsymbol{\sigma}_1 \cdot \mathbf{S}_2) + (\boldsymbol{\tau}_1 \cdot \mathbf{T}_2^\dagger) (\boldsymbol{\sigma}_1 \cdot \mathbf{S}_2^\dagger) + (1 \leftrightarrow 2) \right\} \\ & + \frac{f_{\pi N\Delta}^2}{m_\pi^2} g'_{\Delta\Delta} \left\{ (\mathbf{T}_1 \cdot \mathbf{T}_2^\dagger) (\mathbf{S}_1 \cdot \mathbf{S}_2^\dagger) + (1 \leftrightarrow 2) \right\} . \end{aligned} \quad (6)$$

We fixed $g'_{\Delta\Delta} = 0.5$ [17] since the calculated results depend on it very weakly. Non-locality of mean fields is taken into account by a local effective mass approximation in the form of

$$m^*(r) = m_N - \frac{f_{\text{WS}}(r)}{f_{\text{WS}}(0)} (m_N - m^*(0)) , \quad (7)$$

with the Woods-Saxon radial form $f_{\text{WS}}(r)$.

First we discuss the strength distributions of the GT^- transitions, which are expressed by the GT^\pm response functions for the ground-state $|\Psi_0\rangle$

$$R_{\text{GT}}^\pm(\omega) = \sum_{n \neq 0} |\langle \Psi_n | O_{\text{GT}}^\pm | \Psi_0 \rangle|^2 \delta(\omega - (\mathcal{E}_n - \mathcal{E}_0)) , \quad (8)$$

where $|\Psi_n\rangle$ and \mathcal{E}_n denote the n -th nuclear state and its energy. They are experimentally extracted from the $\Delta J^\pi = 1^+$ cross sections $d^2\sigma_{1^+}(q, \omega)/d\Omega d\omega$ deduced by the multipole decomposition analysis (MDA) as [18]

$$\frac{d^2\sigma_{1^+}(q, \omega)}{d\Omega d\omega} = \hat{\sigma}_{\text{GT}} F(q, \omega) R_{\text{GT}}^\pm(\omega) , \quad (9)$$

with the GT unit cross section $\hat{\sigma}_{\text{GT}}$ and the (q, ω) dependence factor $F(q, \omega)$.

Converting the calculated response functions $R^{\alpha\beta}(\mathbf{r}', \mathbf{r}, \omega)$ into those in the momentum representation $R^{\alpha\beta}(\mathbf{q}', \mathbf{q}, \omega)$, the GT response functions $R_{\text{GT}}^\pm(\omega)$ of Eq. (8) are given by

$$R_{\text{GT}}^\pm(\omega) = \frac{1}{2} \sum_a \left\{ R_{\pm 1, aa}^{NN}(\omega) + 2 \frac{g_A^{N\Delta}}{g_A} R_{\pm 1, aa}^{N\Delta}(\omega) + \left(\frac{g_A^{N\Delta}}{g_A} \right)^2 R_{\pm 1, aa}^{\Delta\Delta}(\omega) \right\} , \quad (10)$$

where $R^{\alpha\beta}(\omega) = R^{\alpha\beta}(\mathbf{q}' = 0, \mathbf{q} = 0, \omega)$. The strength distribution $R_{\text{GT}}^-(\omega)$ from ^{90}Zr to ^{90}Nb was obtained by MDA of the (p, n) data [18, 19], which cover not only the GTGR region but also the excitation energy up to 50 MeV.

Figure 1 shows the g'_{NN} dependence of the GTGR peak position. The curves correspond to the results of $g'_{NN}=0.0-0.9$ in 0.3 steps, with $g'_{N\Delta} = 0.3$ and $m^*(0)/m_N = 0.7$. The result

with $g'_{NN}=0.6$ reproduces the peak position well. This value is very close to the previous results [9, 10]. The excess of the theoretical value around the peaks should be redistributed by the configuration mixing of $2p2h$ states and more [20]. This redistribution is seen as significant experimental strength beyond GTGR. This is the quenching of one kind, which should be distinguished from the other quenching due to Δh mixing discussed below.

Figure 2 examines the $g'_{N\Delta}$ and m^* dependences of the GTGR spectrum. In the left panel the curves denote the results of $g'_{N\Delta}=0.0-0.9$ in 0.3 steps. The peak position hardly depends on $g'_{N\Delta}$ but its height strongly does. Since the $g'_{N\Delta}$ governs the coupling between ph and Δh , it controls how much the GT^- strength in the GTGR region moves up to the Δh region. The m^* dependence is shown in the right panel, where the curves represent the results of $m^*(0)/m_N=1.0-0.6$ in 0.2 steps. The m^* affects the GTGR so weakly that it is hard to get information about m^* . From these analysis, we obtained $g'_{NN} = 0.6 \pm 0.1$ with care for the small $g'_{N\Delta}$ and m^* dependences.

Next we discuss the GT quenching factor Q , which is defined as

$$Q = \frac{S_{GT}^-(\omega_{top}^-) - S_{GT}^+(\omega_{top}^+)}{3(N - Z)}, \quad (11)$$

with

$$S_{GT}^\pm(\omega_{top}^\pm) = \int^{\omega_{top}^\pm} R_{GT}^\pm(\omega) d\omega. \quad (12)$$

Very recently Yako *et al.* [21] applied MDA to both the $^{90}\text{Zr}(p, n)$ and $^{90}\text{Zr}(n, p)$ data, and obtained $Q = 0.88 \pm 0.03$ where they used the end energy $\omega_{top}^- = 57$ MeV (50 MeV of ^{90}Nb excitation) and chose the relevant ω_{top}^+ in account of the Coulomb energy shift.

Since Q is almost exclusively determined by $g'_{N\Delta}$ in the calculation, we display the $g'_{N\Delta}$ dependence in Fig. 3 with fixed $g'_{NN} = 0.6$. The solid line shows the results of the continuum RPA and the dashed line does those of Suzuki-Sakai's formulas [13]. The experimental Q and its uncertainty are shown by the horizontal solid line and the horizontal band, respectively. From this comparison we obtained $g'_{N\Delta} = 0.31 \pm 0.07$. The difference between the present calculation and the Suzuki-Sakai's line is well understood by the mechanism of Arima *et al.* [14].

Third we investigate the enhancement of the pionic modes in the QES region. The relevant spin-longitudinal cross sections ID_q were measured for ^{12}C and ^{40}Ca at $T_p=346$ MeV [5, 6] and 494 MeV [4] taken at RCNP and LAMPF, respectively. We performed

DWIA calculations by use of the response functions $R^{\alpha\beta}(\mathbf{r}', \mathbf{r}, \omega)$, and also estimated the two-step contributions in the same manner as Ref. [6].

Since the obtained characteristics are very similar both for ^{12}C and ^{40}Ca , we compare in Fig. 4 the calculations with the experimental ID_q only for ^{12}C taken at RCNP and LAMPF in the left and right panels, respectively.

The top panels show the g'_{NN} dependence for $g'_{NN}=0.0-0.9$ in 0.3 steps with the fixed $g'_{N\Delta} = 0.3$ and $m^*(0)/m_N = 0.7$. The calculations are sensitive to g'_{NN} near and below the QES peak. The experimental data are reasonably reproduced with $g'_{NN}=0.7$, whose uncertainty could be about 0.1. This result is consistent with the value of $g'_{NN} = 0.6 \pm 0.1$ evaluated from the GTGR spectrum.

The middle panels denote the $g'_{N\Delta}$ dependence for $g'_{N\Delta}=0.0-0.9$ in 0.3 steps with the fixed $g'_{NN} = 0.7$ and $m^*(0)/m_N = 0.7$. The dependence is evidently seen around the QES peak. The most probable choices of $g'_{N\Delta}$ are about 0.4 and 0.2 for the RCNP and LAMPF data, respectively. From these results, we could estimate $g'_{N\Delta} = 0.3 \pm 0.1$, which is consistent with that from the quenching factor Q .

The bottom panels display the m^* dependence for $m^*(0)/m_N=1.0-0.6$ in 0.2 steps with the fixed $g'_{NN} = 0.7$ and $g'_{N\Delta} = 0.3$. The theoretical estimations [22, 23] of $m^*(0)/m_N \approx 0.7$ is consistent with that required by the data.

In summary, we reported the theoretical analyses of the two contrastive phenomena, the quenching of the GT transition and the enhancement of the pionic response at the QES region. The GT strength distributions and the latest data of the quenching factor are calculated by means of the continuum RPA with the $\pi + \rho + g'$ interactions including Δ degree of freedom. In the same framework of the structure calculation incorporated with the DWIA and two-step calculations, we also calculated the spin-longitudinal cross sections ID_p at different incident energies. By this elaborated and comprehensive calculations in a unified way for widespread phenomena, we found a common set of the LM parameters, $g'_{NN}=0.6-0.7$ and $g'_{N\Delta}=0.2-0.4$, which explain the quenching and the enhancement simultaneously.

We thank all the members of the RCNP-E57, E59, E131, and E149 collaborations, especially for K. Yako. This work was supported in part by the Grands-in-Aid for Scientific Research Nos. 12640294, 12740151, and 14702005 of the Ministry of Education, Culture,

- [1] For reviews, see, J. Rapaport and E. Sugarbaker, *Annu. Rev. Nucl. Part. Sci.* **44**, 109 (1994);
W. P. Alford and B. M. Spicer, *Adv. Nucl. Phys.* **24**, 1 (1994).
- [2] C. Gaarde, *Nucl. Phys.* **A396**, 127c (1983).
- [3] C. Gaarde, J. S. Larsen, M. N. Harakeh, S. Y. van der Verf, M. Igarashi, and A. Müller-Arnke,
Nucl. Phys. **A334**, 248 (1980).
- [4] T. N. Taddeucci *et al.*, *Phys. Rev. Lett.* **73**, 3516 (1994).
- [5] T. Wakasa *et al.*, *Phys. Rev. C* **59**, 3177 (1999).
- [6] T. Wakasa *et al.*, *Phys. Rev. C* **69**, 054609 (2004).
- [7] W. M. Alberico, M. Ericson, and A. Molinari, *Nucl. Phys.* **A379**, 429 (1982).
- [8] For a review, see, F. Osterfeld, *Rev. Mod. Phys.* **64**, 491 (1992).
- [9] T. Suzuki, *Phys. Lett.* **104B**, 92 (1981).
- [10] G. Bertsch, D. Cha, and H. Toki, *Phys. Rev. C* **24**, 533 (1981).
- [11] T. Izumoto, *Nucl. Phys.* **A395**, 189 (1983).
- [12] F. Osterfeld and D. Cha and J. Speth, *Phys. Rev. C* **31**, 372 (1985).
- [13] T. Suzuki and H. Sakai, *Phys. Lett. B* **455**, 25 (1999).
- [14] A. Arima, W. Bentz, T. Suzuki, and T. Suzuki, *Phys. Lett. B* **499**, 104 (2001).
- [15] K. Kawahigashi, K. Nishida, A. Itabashi, and M. Ichimura, *Phys. Rev. C* **63**, 044609 (2001).
- [16] K. Nishida and M. Ichimura, *Phys. Rev. C* **51**, 269 (1995).
- [17] W. H. Dickhoff, A. Faessler, J. Meyer-ter-Vehn, and H. Müther, *Phys. Rev. C* **23**, 1154 (1981).
- [18] T. Wakasa *et al.*, *Phys. Rev. C* **55**, 2909 (1997).
- [19] T. Wakasa *et al.*, *J. Phys. Soc. Jpn.* **73**, 1611 (2004).
- [20] G. F. Bertsch and I. Hamamoto, *Phys. Rev. C* **26**, 1323 (1982).
- [21] K. Yako *et al.*, nucl-ex/0411011.
- [22] Nguyen van Giai and Pham van Thieu, *Phys. Lett.* **126B**, 421 (1983).
- [23] C. Mahaux and R. Sartor, *Nucl. Phys.* **A481**, 381 (1988).

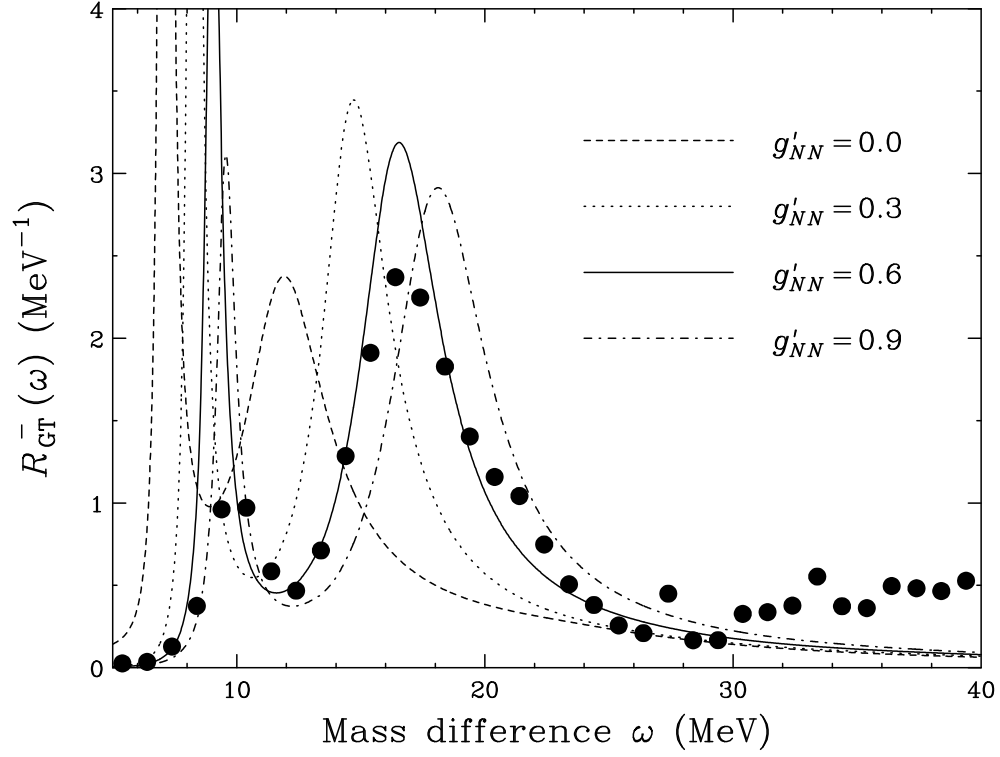


FIG. 1: The g'_{NN} dependence of GT^- strength distributions from ^{90}Zr to ^{90}Nb , where $g'_{N\Delta}$ and $m^*(0)/m_N$ are set to 0.3 and 0.7, respectively. The filled circles are the experimental data taken from Ref. [18].

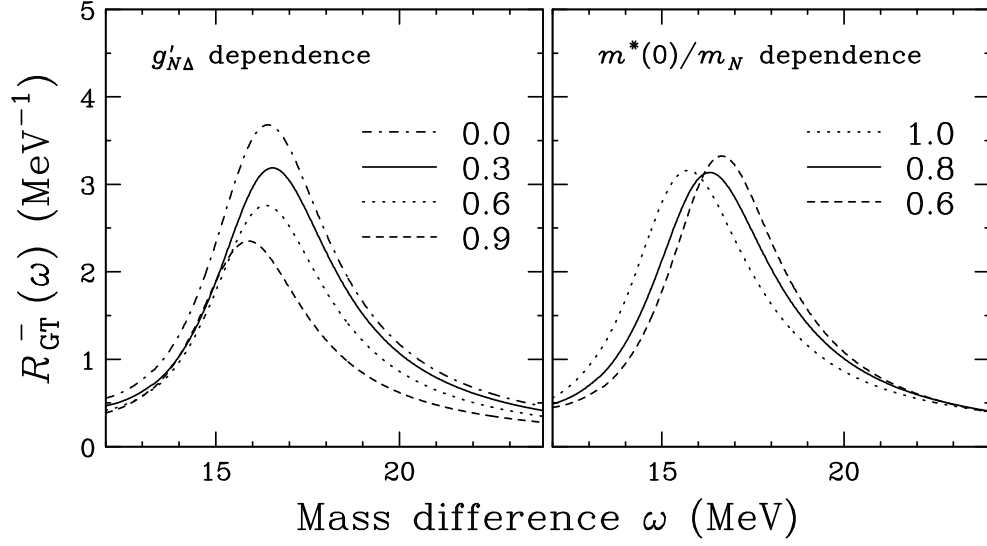


FIG. 2: The $g'_{N\Delta}$ (left panel) and $m^*(0)/m_N$ (right panel) dependences of the RPA calculations. In the left panel g'_{NN} and $m^*(0)/m_N$ are set to 0.6 and 0.7, respectively. In the right panel g'_{NN} and $g'_{N\Delta}$ are set to 0.6 and 0.3, respectively.

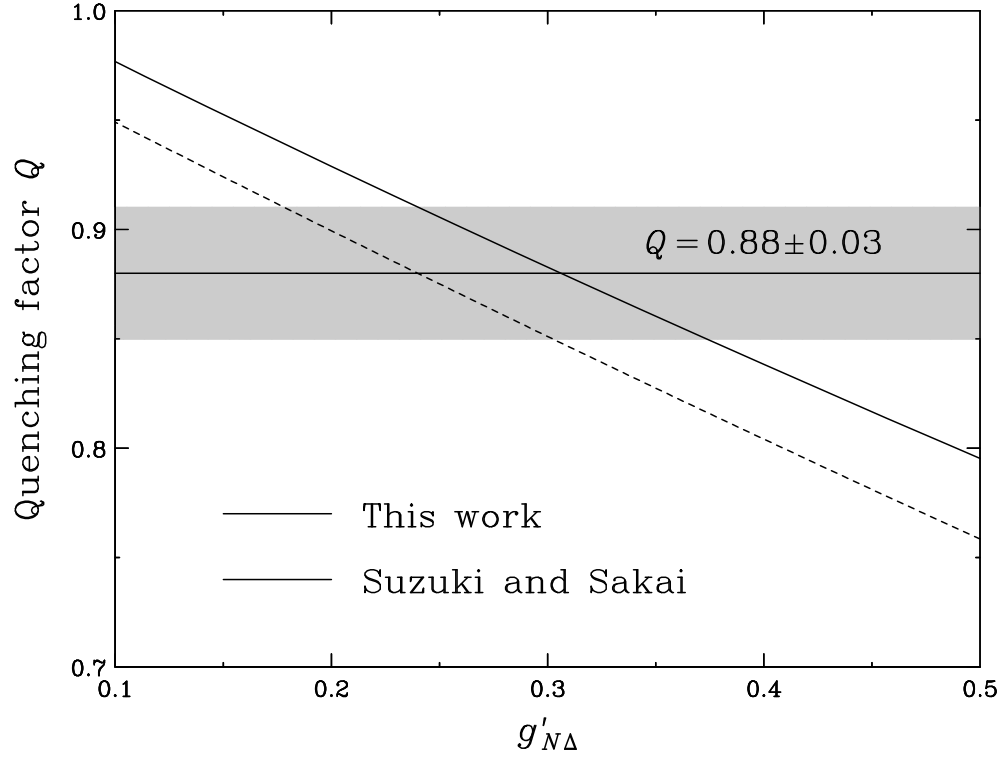


FIG. 3: The GT quenching factor Q as a function of $g'_{N\Delta}$. The experimental result of 0.88 ± 0.03 [21] is shown by the horizontal solid line and band. The dashed curve is the theoretical prediction by Suzuki and Sakai [13].

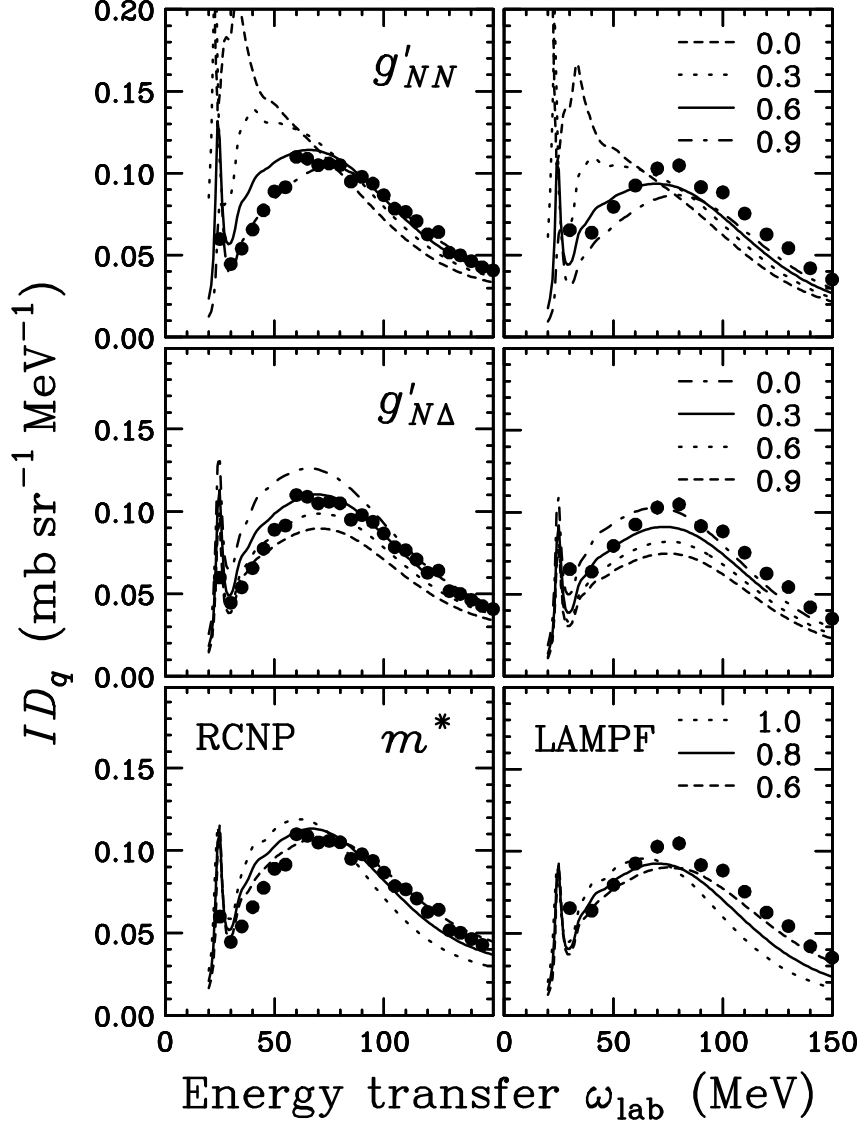


FIG. 4: The spin-longitudinal polarized cross section ID_q for the ^{12}C reaction at $T_p=346$ MeV [5, 6] (left panels) and $T_p=494$ MeV [4] (right panels). The top, middle, and bottom panels show the g'_{NN} , $g'_{N\Delta}$, and $m^*(0)/m_N$ dependences of the calculations. The notations of the curves are the same as those in Figs. 1 and 2 except for $g'_{NN}=0.7$ in the middle and bottom panels.